Cellular and Molecular Life Sciences (2025) 82:217
https://doi.org/10.1007/s00018-025-05734-5

ORIGINAL ARTICLE

α-Ketoglutarate alleviates the pathogenesis of lupus and inhibits the activation and differentiation of B cells by promoting the expression of CD39

Yangzhe Gao[1,2] · Yucai Xiao[1,2] · Yuxin Hu[1,2] · Lu Yu[1,2] · Jiakun Liu[1,2] · Zhengyi Zhang[1,2] · Tianqi Zhao[1,2] · Shuo Zhao[1,2] · Lili Zhang[3] · Yonghong Yang[4] · Huabao Xiong[1,2] · Guanjun Dong[1,2]

Received: 18 November 2024 / Revised: 18 March 2025 / Accepted: 2 May 2025

Abstract

The abnormal activation and differentiation of B cells play an important role in the pathogenesis of autoimmune diseases, including systemic lupus erythematosus (SLE). Alpha-ketoglutarate (α-KG), a key metabolite in the tricarboxylic acid cycle, has been shown to be involved in the pathogenesis of many diseases by regulating the immune response. However, the role of α-KG in the pathogenesis of SLE, as well as the activation and differentiation of B cells, remains unclear. In this study, we used organic acid-targeted metabolomics to analyze the changes in the levels of 100 organic acids in the serum of SLE patients and healthy controls, and found a significant increase in the α-KG level in SLE patients compared to that in healthy controls. Notably, α-KG significantly could inhibit the activation and differentiation of B cells and alleviate disease progression in lupus-prone mice. Mechanistically, RNA-seq revealed that α-KG upregulated the expression of ENTPD1, which encodes an important immune checkpoint molecule CD39; B-cell-specific loss of ENTPD1 could significantly promote the Toll-like receptors-mediated activation and differentiation of B cells and aggravate the disease conditions of lupus-prone mice. The findings of our study demonstrate that α-KG alleviates the pathogenesis of lupus and inhibits the activation and differentiation of B cells by increasing the expression of CD39. Our findings laid a theoretical foundation for understanding the pathogenesis of SLE. Based on our study, α-KG might be further examined as a drug for the effective treatment of SLE.

Keywords Systemic lupus erythematosus · B cells · α-KG · CD39 · Toll-like receptors

Introduction

Systemic lupus erythematosus (SLE) is a systemic and chronic autoimmune disorder that arises from the aberrant activation of the immune system [1]. The pathologic status of SLE is regulated by autoimmune response factors that alter the resident cellular populations in the kidneys and other vital organs, as well as increase the production of autoantibodies found in the systemic circulation, thereby contributing to the progression and manifestation of SLE [2]. Immune cells, such as B cells, macrophages, and dendritic cells (DCs), play crucial roles in the pathogenesis of SLE [3]. Notably, B cells play a central role in the development of SLE, where they orchestrate antigen presentation, produce cytokines, and undergo differentiation into antibody-secreting plasma cells, thus contributing significantly to the disease [4, 5]. Studies have shown that

Yangzhe Gao and Yucai Xiao contributed equally to this work.

✉ Yonghong Yang
healthy_8758@126.com

✉ Huabao Xiong
xionghbl@yahoo.com

✉ Guanjun Dong
guanjun0323@mail.jnmc.edu.cn

1 Institute of Immunology and Molecular Medicine, Jining Medical University, No. 133 Hehua Road, Taibai Lake New Area, Shandong 272067, China

2 Jining Key Laboratory of Immunology, Jining Medical University, Shandong 272067, China

3 Department of Rheumatology, Affiliated Hospital of Jining Medical University, Jining, Shandong 272007, China

4 Medical Research Center, Affiliated Hospital of Jining Medical University, No. 89 Guhuai Road, Rencheng District, Jining, Shandong 272007, China

Published online: 28 May 2025

hyper-activation of B cells increases oxidative phosphorylation-related gene expression and modulates the B-cell lymphoma 6 protein (Bcl-6)–B-lymphocyte-induced maturation protein 1 (Blimp-1) axis, leading to abnormal differentiation of plasma cells and the pathogenesis of lupus [5, 6]. However, the molecular mechanisms that lead to the abnormal activation and differentiation of B cells in SLE are still not fully understood.

As is known, toll-like receptors (TLRs), an evolutionarily conserved family of the innate immune system, are the host's first line of defense against microbial pathogens by recognizing pathogen-associated molecular patterns [7]. After interacting with their respective ligands, TLRs recruit myeloid differentiation factor 88 (MyD88) and lead to the activation of the MAPK and NF-κB signaling pathways [8]. Numerous studies have shown that TLRs play a critical role in regulating the pathogenesis of SLE by regulating the activation and differentiation of immune cells, especially B cells [9, 10]. Germline gain-of-function mutations of TLR7 were shown to cause SLE, highlighting the role of TLR7 in driving autoimmunity [11]. Alterations in TLR signaling thresholds, for example, TLR7 overexpression, exert a B cell–intrinsic contribution to lupus development in mouse and man [12]. TLRs participate in the B-cell tolerance to self-antigens, considering that they orchestrate extrafollicular and germinal center B-cell responses, and are implicated in autoantibody generation and the pathogenesis of SLE [13, 14]. However, the molecular mechanisms leading to the aberrant activation of the TLR signaling pathway in B cells need to be elucidated.

Recent studies have found that metabolism is involved in the regulation of immune response and the pathogenesis of immune-related diseases. Immune cells were found to undergo substantial metabolic alterations during their activation and differentiation, characterized by an increase in energy demands and faster synthesis of essential biological building blocks, indicating that metabolism plays a key role in regulating the activation and differentiation of immune cells [15, 16]. Notably, in recent years, more and more attention has been paid to the role of organic acids, which actively participate in biochemical reactions in the body, in maintaining immune homeostasis. Among organic acids, α-ketoglutarate (α-KG) is an important metabolite in the tricarboxylic acid cycle (TCA), where it performs crucial functions [17, 18]. It has been shown that α-KG plays antiviral, antitumor, and anti-inflammatory roles by modulating the activation and differentiation of immune cells [19–21]. Exogenous α-KG modulates redox metabolism and functions of dendritic cells (DCs), altering their capacity to polarise T cell response [22]. Dietary α-KG can alleviate LPS-induced intestinal inflammation through the T helper 17 cells (Th17)/Regulatory T cells (Treg) immune response signaling pathway [23]. Also, α-KG can restore the function of T cells by facilitating ammonia detoxification in $CD8^+$ T cells, thereby increasing their antiviral efficacy [24]. Of note, several studies have shown that α-KG can exert its immunomodulatory function by causing DNA hypermethylation to regulate gene expression [25, 26]. Although α-KG participates in various cellular metabolic processes and the regulation of inflammatory cells and inflammatory factors, the effects of α-KG on the development of lupus remain unknown. Moreover, the roles of α-KG on the activation and differentiation of B cells are still unknown.

In this study, we investigated the role of α-KG in regulating the activation and differentiation of B cells as well as the pathogenesis of lupus. Compared with healthy controls, patients with SLE showed significantly higher levels of α-KG in the serum. Interestingly, α-KG significantly inhibited the TLR-mediated activation and differentiation of B cells and alleviated disease progression in lupus-prone mice by increasing the expression of ectonucleoside triphosphate diphosphohydrolase-1 (ENTPD1), which encodes the immune checkpoint CD39. Additionally, B-cell-specific loss of ENTPD1 significantly promoted the TLR-mediated activation and differentiation of B cells and aggravated the disease conditions of lupus-prone mice. Our findings indicated that α-KG can alleviate the pathogenesis of lupus and inhibit the activation and differentiation of B cells by promoting CD39 expression. Our study highlighted that α-KG is a promising candidate for treating SLE and should be further investigated.

Materials and methods

Animals

C57BL/6 mice, aged 6 to 8 weeks, were procured from Pengyue Experimental Animal Breeding Co. (Jinan, China). MRL/*lpr* mice, specifically 10 weeks old, were sourced from Jiangsu Aniphe Biolaboratory, Inc. They were acclimatized in the animal facilities of Jining Medical University for 2–3 weeks before conducting the experiment. ENTPD1$^{fl/fl}$ mice on a C57BL/6 background were generated using a LoxP-targeting system at the Cyagen Biosciences. The ENTPD1$^{fl/fl}$ mice were crossed with CD19-Cre transgenic mice (Cyagen Biosciences) on a B6 background to obtain age-matched ENTPD1$^{\Delta CD19}$ mice for experiments. All mice were housed in pathogen-free conditions specific to Jining Medical University, in accordance with the ARRIVE guidelines, the 12 h/12 hr light/dark cycle followed, and fed standard chow.

To investigate the impact of α-KG (Selleck) on the pathogenesis of MRL/*lpr* mice, MRL/*lpr* mice (thirteen-week-old,

female) were randomly assigned to two distinct groups, each comprising six animals. One group served as vehicle group, while the other group underwent intraperitoneal injections of α-KG at a dosage of 75 μg/g three times weekly. Subsequently, after 4 weeks of treatment, the mice were euthanized via CO_2 inhalation, and the spleens and lymph nodes were subjected to testing for the presence of the desired indicators.

To establish an IMQ-induced lupus mouse model, female C57BL/6 mice were topically administered with 1.25 mg of 5% imiquimod cream (IMQ, sourced from Sichuan MEDSHINE Pharmaceutical Co., Ltd.) to their right ear on a three-times-weekly basis for 10 weeks. To investigate the therapeutic potential of α-KG in IMQ-induced lupus mice, female C57BL/6 mice were randomly allocated into five groups, each containing six mice. Group A served as vehicle group. Group B was administered α-KG (100 μg/g, intraperitoneally), also serving as a control. Group C applied IMQ to the skin of the right ear only. Group D was treated with IMQ application and α-KG (50 μg/g, intraperitoneally), and Group E received IMQ application with α-KG (100 μg/g, intraperitoneally). Injections of α-KG in mice were performed three times a week for a total of 10 weeks.

To investigate the impact of CD39 on IMQ-induced lupus in mice, the animals were stratified into four groups: Group A comprised $ENTPD1^{fl/fl}$ mice serving as a control, Group B contained $ENTPD1^{\Delta CD19}$ mice serving as an additional control, Group C encompassed $ENTPD1^{fl/fl}$ mice exposed to IMQ, and Group D consisted of $ENTPD1^{\Delta CD19}$ mice subjected to IMQ. The IMQ-treated groups received a topical application of IMQ three times weekly. After a 10-week treatment period, the mice were euthanized via CO_2 inhalation, and the desired indices were assessed.

Information on patients and healthy donors

Prior to their participation, all patients diagnosed with SLE and healthy individuals provided written informed consent. All patients were diagnosed in accordance with the revised criteria established by the American College of Rheumatology (1997), and disease activity was assessed utilizing the SLE Disease Activity Index (SLEDAI). A threshold value of 5 or higher on the SLEDAI scale was utilized to define the presence of active disease. Patients receiving high-dose immunocytotoxic therapeutic drugs or steroids, as well as those with overlapping syndromes, were excluded from the study. Peripheral blood samples were collected from both SLE patients and healthy donors.

Isolation of human peripheral blood mononuclear cells (PBMCs)

Peripheral blood mononuclear cells (PBMCs) were isolated from blood samples, which were collected in heparinized tubes from both SLE patients and healthy donors, utilizing Ficoll-Paque™ PLUS (GE Healthcare) as the separation medium.

Isolation of murine Splenic Naïve B cells

Murine spleens underwent mechanical disruption to obtain a cell suspension, and naïve B cells were subsequently isolated using the Mouse B Cell Isolation Kit (BD Biosciences). This negative selection method ensured a purity of B cells exceeding 95%. The sorted B cells were then cultured in complete RPMI 1640 medium, stimulated with LPS (100 ng/ml, Beyotime), R848 (1 μg/mL, GlpBio), and CpG-1826 (1 μM, Invitrogen), followed by treatment with α-KG (0, 0.25, 0.5, 1, 2.5, and 5 mM) for 18 h. The activation and differentiation of B cells was then assessed by flow cytometry.

RNA-seq analysis

Murine B cells were harvested by TRIzol and sent to Genesky Technologies for analysis. Samples were sequenced on an Illumina HiSeq 2500 instrument using 2 × 150 bp reads. Protein-coding genes with at least 2 RPKM (reads per kilobase of transcript, per million mapped reads) on average in either condition were used to perform the differential gene expression analysis using edgeR. The common genes were further undergoing KEGG pathway enrichment analysis. The data from this study have been deposited in the China National GeneBank (CNGB) Nucleotide Sequence Archive (CNSA) (https://db.cngb.org/cnsa/) with accession number CNP0007013.

Preparation of bone marrow derived macrophages and dendritic cells

Bone marrow cells were extracted from the tibia and femur of C57BL/6 mice for the culturing of BMDMs and BMDCs. BMDMs were cultured in complete DMEM medium supplemented with GM-CSF (10 ng/mL, Peprotech), while BMDCs were cultured in complete RPMI 1640 medium containing both GM-CSF (10 ng/mL) and IL-4 (1 ng/mL). After treating the cells with α-KG for 18 h and then stimulating the cells with LPS (100 ng/ml, Beyotime), R848 (1 μg/mL, GlpBio), and CpG-1826 (1 μM, Invitrogen) for 18 h, BMDMs and BMDCs were harvested and the desired experimental indexes were determined.

Real-time quantitative PCR

Total RNA was extracted from the samples using Trizol reagent (Invitrogen, Carlsbad, USA), following the manufacturer's protocol. Subsequently, cDNA was synthesized from the extracted RNA using the RevertAid First Strand cDNA Synthesis Kit (ThermoFisher Scientific). Quantitative PCR (Q-PCR) analysis was then performed using SYBR Green PCR Master Mix (Vazyme Biotech). The relative gene expression levels were calculated using the $2^{-\Delta\Delta Ct}$ method, with GAPDH serving as the internal reference control for normalization.

H&E staining

Mouse kidneys were first stabilized and fixed in a 4% paraformaldehyde solution for 24 h. Following fixation, the tissues underwent dehydration through a series of increasingly concentrated ethanol solutions and were then embedded in paraffin. From the paraffin-embedded tissue blocks, ultrathin sections of 4 micrometers in thickness were precisely cut. These sections were then stained with hematoxylin and eosin (H&E) staining solution, enabling their visualization under a light microscope (Nikon Corporation). A blinded, semiquantitative assessment method was employed to evaluate the degree of proliferation in the glomerular cells.

Targeted organic acid metabolomics

Samples were thawed and stored at -80 °C, vortexed, extracted in an ice-water bath and centrifuged by adding 240 μL of methanol-acetonitrile containing seven isotopic internal standards. The supernatant was derivatized with methoxylamine hydrochloride and BSTFA, followed by gas chromatography-mass spectrometry (GC-MS) analysis (Thermo Scientific TSQ9000) using a DB-5MS column and helium carrier gas, and mass spectrometry analysis using an EI with SRM.

Immunofluorescence staining

To prepare kidney tissue sections for immunofluorescence staining, the sections were first deparaffinized and rehydrated through a series of washes with xylene and ethanol. Nonspecific binding was then blocked using 1% BSA. The tissue sections were subsequently incubated with Alexa Fluor 488-labeled goat anti-mouse IgG or IgM antibodies (Invitrogen) at 4 °C overnight. The next day, the sections were washed with PBST. The sections were then stained with DAPI to visualize the nuclei. Following staining, the tissue sections were mounted on coverslips using an antifade sealer (Beyotime) and sealed with an antifade bursting agent to prevent fading of the fluorescent signal. Finally, the sections were examined under a confocal fluorescence microscope (Olympus, Japan).

Flow cytometer

For cellular phenotypic staining analysis, cells are first collected and prepared into a homogeneous single-cell suspension, and then stained with specific flow cytometry-compatible antibodies. To perform cell surface labeling staining, cells were first collected and processed into a single-cell suspension. Subsequently, the cells were stained with antibodies specific for the desired phenotypes. The staining process involved incubating the cells with the antibodies for 30 min at 4 °C in the dark. After staining, the cells were washed by PBS and analyzed by flow cytometry.

For intracellular labeling staining, prepared cell suspensions were initially stained with antibodies specific to cell surface markers. Following this, the cells were fixed using an intracellular (IC) fixation buffer (eBioscience). After fixation, the cells were washed and then subjected to intracellular staining using specific antibodies (TNF-α and IL-12) to the cytokines in 100 μl permea-bilization buffer. The cells were incubated overnight at 4 °C in the dark. The next day, the cells were washed with PBS to remove unbound antibodies before being analyzed. Analysis was performed using a BD FACSVerse™ instrument and all FACS data were processed using Flowjo software. To ensure accurate results, isotype controls were included for each antibody used in the analysis.

ELISA

The concentrations of TNF-α and IL-12 p40 in BMDMs and BMDCs supernatants were quantitatively assessed utilizing a mouse-specific ELISA kit sourced from Biolegend. In brief, the ELISA protocol involved an overnight incubation of samples with Capture Antibody, followed by non-specific blocking with 1% BSA the subsequent day. Subsequently, the samples were added for oscillatory incubation. This was followed by the addition of Avidin-HRP solution. To visualize the reaction, 100 μl of TMB color solution was added, resulting in a chromogenic reaction. The reaction was terminated by the addition of 100 μl of termination solution. Finally, the absorbance of each sample was measured at 450 nm using a microplate reader (BioTek).

To quantify anti-dsDNA antibody levels, we performed a standard assay utilizing a mouse anti-dsDNA IgG kit (Bethyl Laboratories). Specifically, we analyzed the concentrations of IgG antibodies targeting dsDNA in the serum of MRL*/lpr* mice and IMQ-induced lupus-prone mice. Following the manufacturer's instructions, the absorbance of

each sample at 450 nm was accurately measured using a BioTek zymography instrument.

Western blot

In summary, cells were harvested and subjected to lysis with an appropriate buffer. Subsequently, the protein concentration in these homogenates was accurately determined using a BCA protein assay kit from Beyotime. Proteins were resolved by 10% SDS-PAGE and subsequently transferred onto a 0.45 μm PVDF membrane sourced from Millipore. To minimize non-specific binding, the membrane was blocked with 5% BSA for 2 h at room temperature. Following blocking, the membrane was incubated overnight at 4 °C with the primary antibody of interest. The next day, the membrane underwent five thorough washes, and then was incubated with a HRP-conjugated secondary antibody (Beyotime) for 2 h at room temperature. Protein expression was visualized using an enhanced chemiluminescence (ECL) kit provided by Biosharp. To ensure the accuracy and reproducibility of the results, β-actin was utilized as an internal control.

Antibodies

The following antibodies were used for immunoblotting: Cell Signaling Technology, anti-Erk (Cat#: 4695), anti-p-Erk (Cat#: 4370), anti-JNK (Cat#: 9252), anti-p-JNK (Cat#: 4668), anti-p38 (Cat#: 8690), anti-p-p38 (Cat#: 4511), anti-p65 (Cat#: 8242), anti-p-p65 (Cat#: 3033); Beyotime Institute of Biotechnology, anti-β-actin (Cat#: AA128), HRP labeled Goat Anti-Rabbit IgG (Cat#: A0208), HRP-labeled Goat Anti-Mouse IgG (Cat#: A0216). The following antibodies purchased from Biolegend were used for flow cytometry: FITC anti-mouse B220 (Cat#: 103206), PE anti-mouse GL7 (Cat#: 144607), PE anti-mouse CD40 (Cat#: 124610), APC anti-human CD86 (Cat#: 374208), BV421 anti-mouse CD11c (Cat#: 117330), FITC anti-mouse F4/80 (Cat#: 123108), APC anti-mouse CD86 (Cat#: 105012), APC anti-mouse CXCR5 (Cat#: 145506), PE anti-mouse PD-1 (Cat#: 135206), APC anti-mouse CD138 (Cat#: 142506), BV421 anti-mouse CD69 (Cat#: 104528), FITC anti-mouse CD4 (Cat#: 100406), BV421 anti-mouse CD62L (Cat#: 104436), PE anti-mouse CD44 (Cat#: 103007), PE anti-mouse CD39 (Cat#: 143804), APC anti-mouse CD39 (Cat#: 143809), APC anti-mouse CD95 (Cat#: 152604). All the antibodies for flow cytometry were used at a 1:100 dilution.

Statistical analyses

For the statistical analysis of our data, we relied on GraphPad Prism software. To evaluate differences between groups, we employed both Two-tailed unpaired Student's *t*-test and one-way ANOVA analysis, depending on the nature of the comparisons. For assessing the relationship between paired datasets, we utilized Pearson's correlation analysis. Throughout our analysis, we considered a *p*-value of less than 0.05 as statistically significant.

Results

High levels of α-KG in the serum of SLE patients and lupus model mice

Using organic acid-targeted metabolomics, we analyzed the content of 100 organic acids and the percentage of multiple organic acids in the serum of nine SLE patients and nine healthy controls (Fig. 1a). The levels of seven organic acids, such as α-KG, DL-β-phenyllactic acid, and 3-hydroxyisovaleric acid, were significantly greater in the serum of SLE patients than in the serum of healthy controls (Fig. 1b, S1a). However, the levels of seven organic acids, such as isophthalic acid, lactic acid, and itaconic acid, were significantly lower in the serum of SLE patients than in the serum of healthy controls (Fig. 1b, S1b). Notably, α-KG plays a broad role in regulating the pathogenesis of various diseases, but its effect on the development of SLE is unknown. Therefore, α-KG has attracted considerable research interest. Serum samples from 26 healthy controls, 15 inactive SLE patients, and 54 active SLE patients were collected, and the levels of α-KG were measured. The level of α-KG was significantly greater in active SLE patients than in healthy controls and nonactive SLE patients (Fig. 1c). Additionally, the serum α-KG levels were significantly greater in MRL/*lpr* spontaneous lupus mice (Fig. 1d) and IMQ-induced lupus-prone mice (Fig. 1e) than in WT mice. These results indicated that the serum α-KG content was significantly higher in SLE patients and lupus model mice, suggesting that α-KG may play an important regulatory role in the occurrence and development of lupus.

α-KG alleviated lupus symptoms in MRL/*lpr* mice and inhibited the activation and differentiation of B cells

To determine the effect of α-KG on the onset of lupus, we first investigated the effect of α-KG on the onset of spontaneous lupus in MRL/*lpr* mice. Compared to vehicle-treated MRL/*lpr* mice, α-KG-treated MRL/*lpr* mice presented significantly less spleen enlargement (Fig. 2a), which was characterized by a decrease in spleen size and weight (Fig. 2b) and a reduction in serum anti-dsDNA antibody levels (Fig. 2c). An examination of H&E-stained sections revealed that α-KG treatment significantly reduced kidney

a

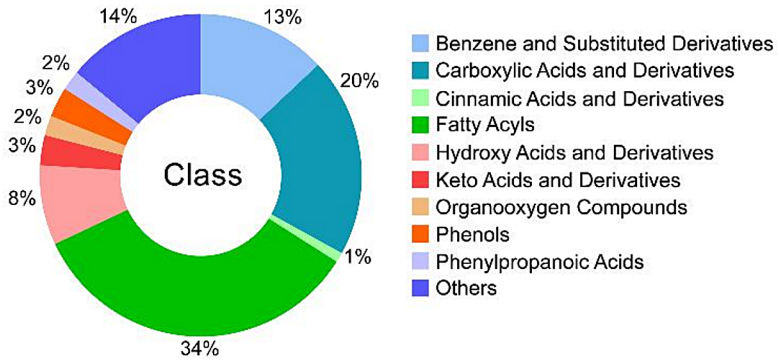

b

Metabolites	HC (Average)	SLE (Average)	P-value	Change
α-Ketoglutaric acid (α-KG)	746.14	1093.99	P=0.0370	Up
L-phenylalanine	4015.81	5223.70	P=0.0309	Up
DL-pyroglutamic acid	5858.44	8030.68	P=0.0034	Up
L-2-hydroxyglutaric acid disodium	62.27	87.81	P=0.0292	Up
3-hydroxyisovaleric acid	8.67	18.66	P=0.0185	Up
DL-Beta--phenyllactic acid	16.67	29.79	P=0.0046	Up
Glycine	1310.95	2245.64	P=0.0009	Up
Uracil	50.83	12.89	P<0.0001	Down
Isophthalic acid	36.84	33.00	P=0.0085	Down
Lactic acid	338999.83	274126.29	P=0.0286	Down
Itaconic acid	11.46	7.54	P=0.0356	Down
Benzoic acid	104.67	82.20	P=0.0379	Down
N-acetylglycine	14688.36	10412.18	P=0.0393	Down
Pentadecanoic acid	611.83	255.13	P=0.0248	Down

c

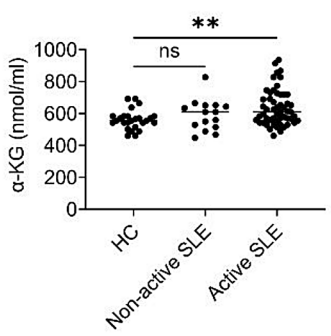

d

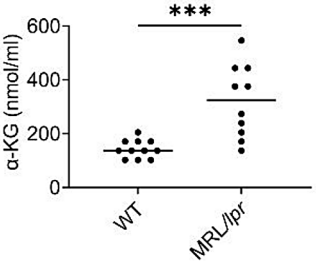

e

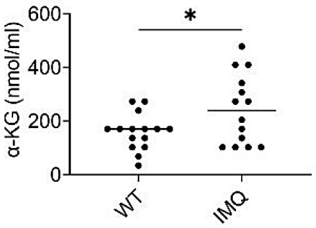

Fig. 1 The content of α-KG in serum of SLE patients and lupus-prone mice is abnormally increased **a** The classes of 100 organic acids by organic acid-targeted metabolomics. **b** Comparative analysis of the mean serum levels of organic acid metabolites, including α-KG, between the healthy control group ($n=9$) and the SLE patient group ($n=9$), with calculation of p-values and elaboration on the alterations in organic acid levels in SLE patients compared to healthy donors. **c** Measurement of α-KG levels in the peripheral blood serum of healthy donors ($n=26$), inactive SLE patients ($n=15$), and active SLE patients ($n=54$). **d** Measurement of α-KG levels in the serum of wild-type (WT) mice ($n=11$) and MRL/*lpr* mice ($n=10$). **e** Measurement of α-KG levels in the serum of IMQ-induced lupus mice ($n=14$) compared to control mice ($n=15$). The data are shown as the means ± SEM and are representative of three independent experiments. *$p<0.05$, **$p<0.01$, and ***$p<0.001$ (two-tailed Student's t-test or ANOVA tests)

injury in MRL/*lpr* mice (Fig. 2d), and confocal immunofluorescence analysis revealed a significant reduction in the deposition of IgG and IgM in the glomerulus of α-KG-treated MRL/*lpr* mice than in the glomerulus of vehicle-treated MRL/*lpr* mice (Fig. 2e). These results indicated that exogenous α-KG can significantly alleviate the disease in MRL/*lpr* lupus model mice.

We also analyzed the effects of α-KG on the activation and differentiation of immune cells in the spleens and mesenteric lymph nodes (mLNs) of MRL/*lpr* mice. Compared to vehicle-treated MRL/*lpr* mice, α-KG-treated MRL/*lpr* mice presented significantly lower expression of CD86 on the surface of $B220^+$ B cells (Fig. 2f, g), a lower proportion of germinal center (GC) B cells (Fig. 2h, i) and plasma cells (Fig. 2j, k) in the spleens and mLNs, which indicated that α-KG significantly inhibited the activation and differentiation of B cells in vivo. Since T cells, macrophages, and DCs also play important roles in the pathogenesis of lupus, we assessed the effects of α-KG on the activation and differentiation of these cells in MRL/*lpr* mice. We found that α-KG treatment significantly inhibited the expression of CD69 on the surface of $CD4^+$ T cells (Fig. S2a, S2b) and decreased the proportions of follicular helper T (Tfh) cells (Fig. S2c, S2d) in the spleens and mLNs and memory $CD4^+$ T cells (Fig. S2e) in the spleens. Additionally, α-KG treatment significantly inhibited the expression of CD86 and CD40 on the surface of macrophages (Fig. S2f, S2g) and DCs (Fig. S2h, S2i). These results indicated that α-KG strongly inhibits the activation and differentiation of immune cells, such as B cells and T cells *in vivo*.

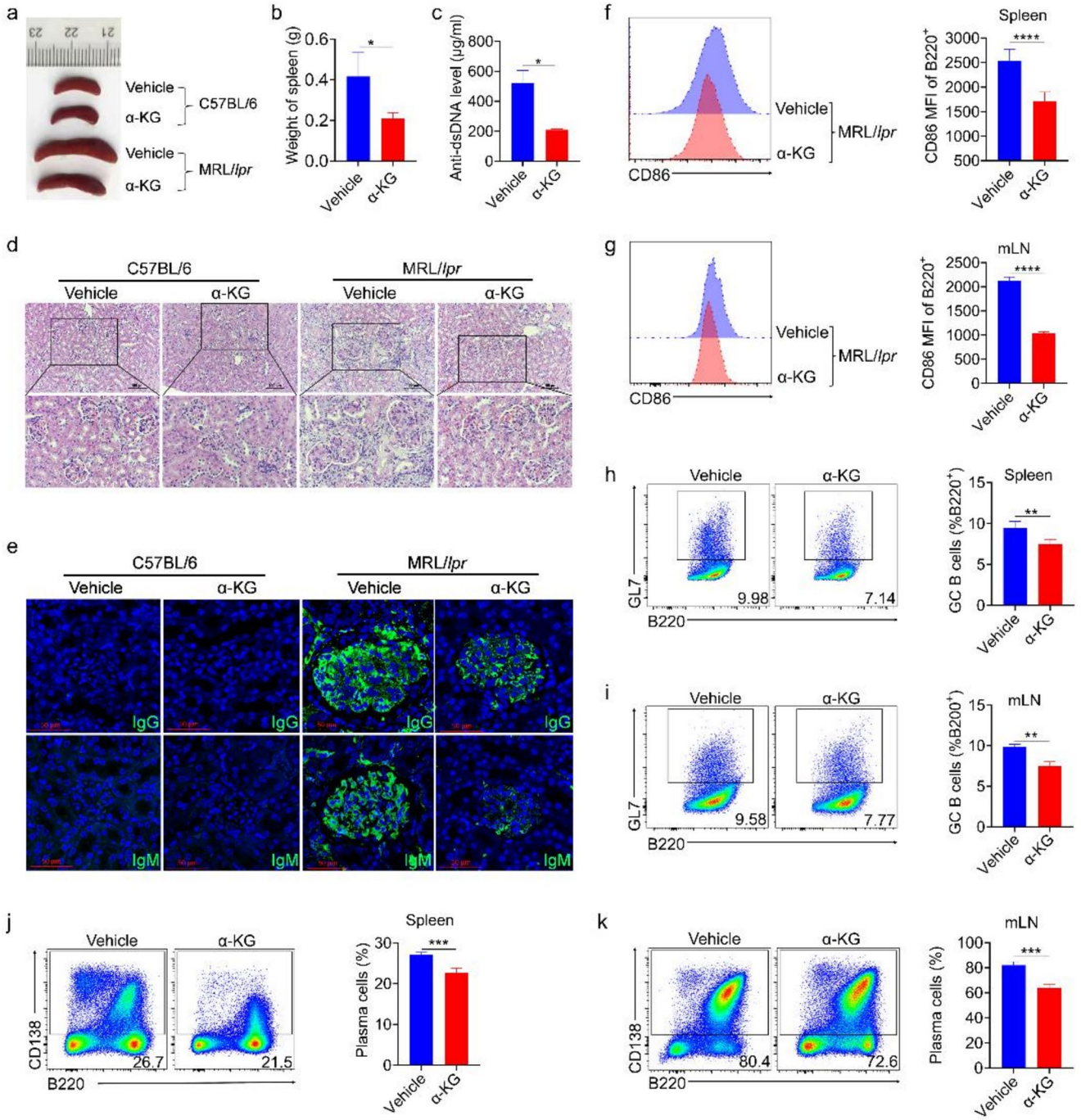

Fig. 2 α-KG significantly mitigates the disease progression in MRL/lpr lupus-prone mice MRL/*lpr* lupus mice (female, thirteen-week-old) were treated with α-KG (75 μg/g, intraperitoneally) or vehicle for four weeks (three times per week). **a** Representative images of spleen morphology, **b** spleen weights, **c** serum levels of anti-dsDNA antibody, **d** H&E staining of kidney tissue, and **e** renal IgG and IgM deposition in MRL/*lpr* lupus mice treated with α-KG (75 μg/g) or vehicle. Scale bars represent 100 μm. **f-k** Flow cytometry analysis was conducted to assess the expression of CD86 on $B220^+$ B cells (**f**, **g**), the percentage of GC B cells ($B220^+GL7^+$) in $B220^+$ B cells (**h**, **i**), and the percentage of plasma cells ($CD138^+$) (**j**, **k**) in the spleens and mLNs. The data are shown as the means ± SEM and are representative of three independent experiments ($n = 6$ mice/group). $^*p < 0.05$, $^{**}p < 0.01$, and $^{****}p < 0.0001$ (two-tailed Student's *t*-test or ANOVA tests)

α-KG alleviated lupus symptoms in TLR7 agonist IMQ-induced lupus model mice and inhibited the activation and differentiation of B cells

Next, we investigated the effect of α-KG on the onset of the TLR7 agonist IMQ-induced lupus in mice (IMQ mice) (Fig. 3a). Consistent with the above results, compared to vehicle-treated IMQ mice, A notable decrease in spleen size and weight was observed in IMQ mice subjected to α-KG treatment (Fig. 3b, c), as well as lower levels of serum anti-dsDNA antibodies (Fig. 3d). Additionally, α-KG treatment greatly reduced kidney injury (Fig. 3e) and the deposition of IgG and IgM in the glomerulus (Fig. 3f) of IMQ mice. These results indicated that exogenous α-KG can also significantly alleviate the disease in IMQ lupus-prone mice.

The effects of α-KG on the activation and differentiation of immune cells in IMQ-treated mice were analyzed. As shown in Fig. 3, α-KG treatment significantly reduced the expression of CD86 in spleens (Fig. 3g, h) and mLNs (Fig. S3a, S3b) on the surface of $B220^+$ B cells, the proportions of GC B cells (Fig. 3i and j, S3c, and S3d) and plasma cells (Fig. 3k and l, S3e, and S3f), indicating that α-KG significantly inhibited the activation and differentiation of B cells in spleens and mLNs. Moreover, α-KG treatment significantly inhibited the expression of CD69 on the surface of $CD4^+$ T cells (Fig. S4a, S4b) and decreased the proportions of Tfh (Fig. S4c, S4d) cells in spleens and mLNs and memory $CD4^+$ T cells (Fig. S4e) in spleens. Additionally, α-KG treatment significantly inhibited the expression of CD86 and CD40 on the surface of macrophages(Fig. S4f, S4g) and DCs (Fig. S4h, S4i) in the spleens. These results indicated that α-KG strongly regulates the activation and differentiation of immune cells such as B cells and T cells.

α-KG inhibited the activation of the TLR signaling pathway in B cells in vitro

As TLR-mediated abnormal activation and differentiation of B cells play key roles in the pathogenesis of lupus, we investigated whether α-KG can modulate the TLR-mediated activation of B cells in vitro. First, we conducted a series of experiments to assess the effects of various concentrations of α-KG on the apoptosis of murine splenic naïve B cells and found that <5 mM α-KG had negligible effects on B-cell apoptosis (Fig. S5a-c). Thus, we ensured that none of the subsequent in vitro experiments exceeded this concentration threshold. Next, murine naïve B cells were pretreated with various concentrations of α-KG and then stimulated with the specific TLR4 agonist LPS, the TLR7 agonist R848, and the TLR9 agonist CpG-1826. Consistent with our in vivo findings, pretreatment with α-KG significantly suppressed the TLR ligand-induced upregulation of CD86 and CD40 expression on the surface of B cells with LPS (Fig. 4a, b), R848 (Fig. 4c, d), and CpG-1826 (Fig. 4e, f) in a concentration-dependent manner. Moreover, α-KG strongly suppressed the TLR ligand-induced Secretion of TNF-α (Fig. 4g) and IL-12 (Fig. 4h) in B cells in a concentration-dependent manner. Additionally, α-KG markedly inhibited TLR-induced phosphorylation of p38, Erk, JNK, and p65 in B cells (Fig. 4i). These findings indicated that α-KG can effectively decrease the activation of TLR signaling pathways in B cells in vitro.

To confirm the effect of α-KG on the activation of TLR signaling pathways, we also assessed its effect on TLR-induced activation of macrophages and DCs. By pretreating BMDMs and BMDCs with different concentrations of α-KG before stimulation with LPS, R848, or CpG-1826, we found significant and concentration-dependent inhibition of TLR ligand-mediated upregulation of CD86 and CD40 expression on the surface of these cells (Fig. S6a-f, S7a-f). Moreover, α-KG strongly suppressed the TLR ligand-induced secretion of TNF-α and IL-12 p40 from BMDMs (Fig. S6g, S6h) and BMDCs (Fig. S7g, S7h) in a concentration-dependent manner. These findings highlighted that α-KG can inhibit the activation of TLR signaling pathways in various immune cell types.

α-KG inhibited the activation of TLR pathways by increasing CD39 expression

To elucidate the mechanism by which α-KG inhibits the activation of TLR pathways, RNA-seq was performed to analyze α-KG-regulated gene expression in B cells (Fig. 5a). The results of the KEGG signaling pathway enrichment analysis showed that the DEGs were associated mainly with metabolism-related pathway, including ascorbate and aldarate metabolism, retinol metabolism, pentose and glucuronate interconversion and so on (Fig. 5b). Notably, the RNA-seq data suggested that treatment with α-KG upregulated the expression of ENTPD1, the gene encoding the immune checkpoint molecule CD39 (Fig. 5c). To confirm the effect of α-KG on ENTPD1/CD39 expression on B cells, murine splenic B cells were treated with α-KG for different durations, and ENTPD1/CD39 expression was detected by conducting qPCR and flow cytometry assays. As shown in Fig. 5d and e, α-KG could upregulate the expression of ENTPD1/CD39 on B cells in vitro. To further substantiate the regulatory impact of α-KG on the expression of CD39 on B cells in vivo, we examined the expression of CD39 on B cells from the mice treated with α-KG. As expected, α-KG could also markedly upregulate the expression of CD39 on B cells in vivo (Fig. 5f-i).

CD39, also known as extracellular NTPDase 1, plays an important inhibitory function in the regulation of immune

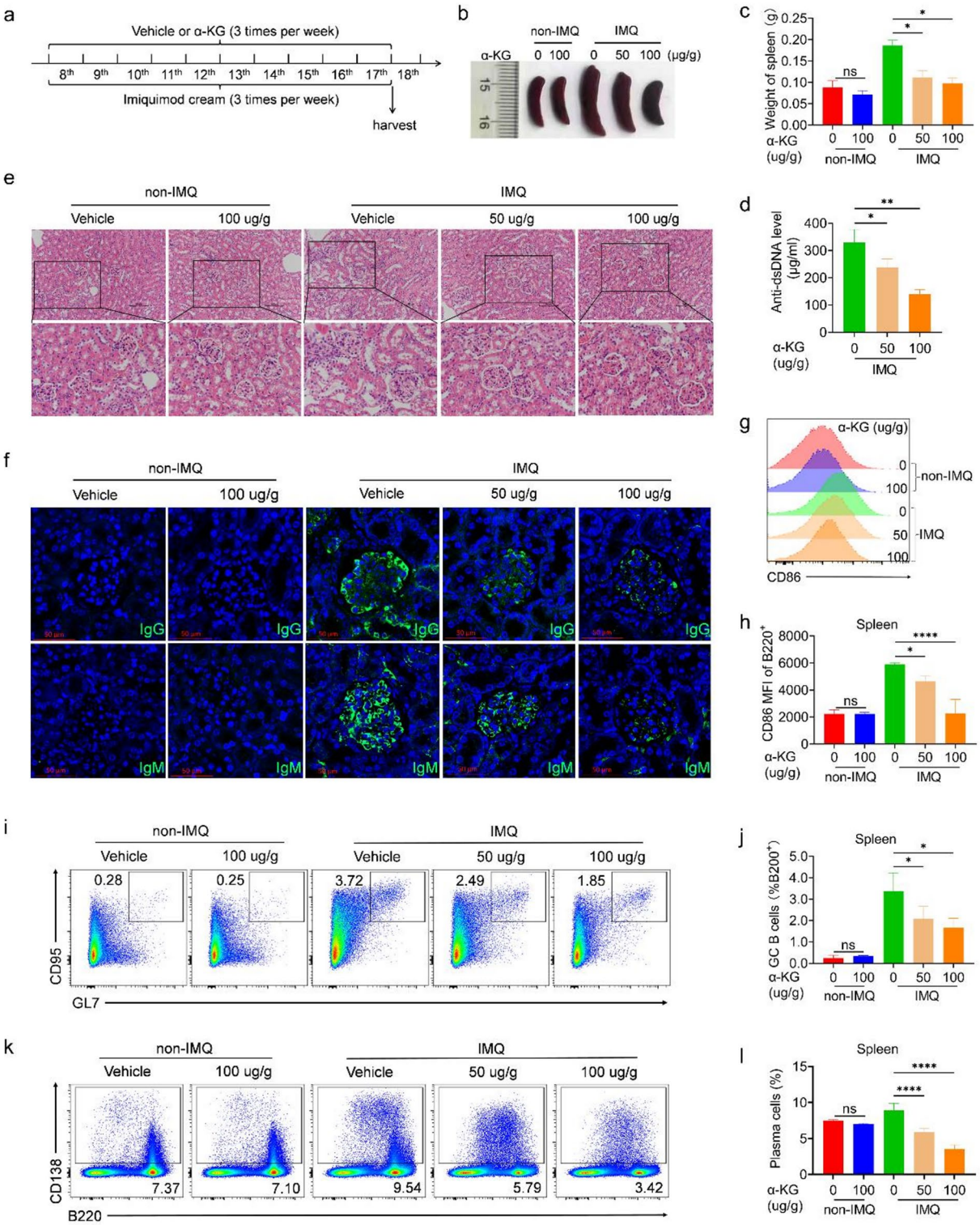

Fig. 3 α-KG significantly alleviates the disease progression in IMQ-induced lupus-prone mice IMQ-induced lupus-prone mice (female, eight-week-old) were treated with α-KG (50 and 100 μg/g, intraperitoneally) or vehicle for ten weeks (three times per week). **a** The diagram shows the treatment process of IMQ-treated WT mice injected with vehicle or α-KG (50 and 100 μg/g, intraperitoneally). **b** Representative images of spleen morphology, **c** spleen weights, **d** serum levels of anti-dsDNA antibody, **e** H&E staining of kidneys, and **f** renal IgG and IgM deposition in IMQ-induced lupus-prone mice treated with α-KG (50 and 100 μg/g, intraperitoneally) or vehicle. Scale bars represent 100 μm. **g-l** Flow cytometry analysis was conducted to determine the expression of CD86 on $B220^+$ B cells (**g**, **h**), the percentage of GC B cells ($B220^+GL7^+CD95^+$) in $B220^+$ B cells (**i**, **j**), and the percentage of plasma cells ($CD138^+$) (**k**, **l**) in the spleens. The data are shown as the means ± SEM and are representative of three independent experiments ($n = 6$ mice/group). $^*p < 0.05$, $^{**}p < 0.01$, and $^{****}p < 0.0001$ (two-tailed Student's *t*-test or ANOVA tests)

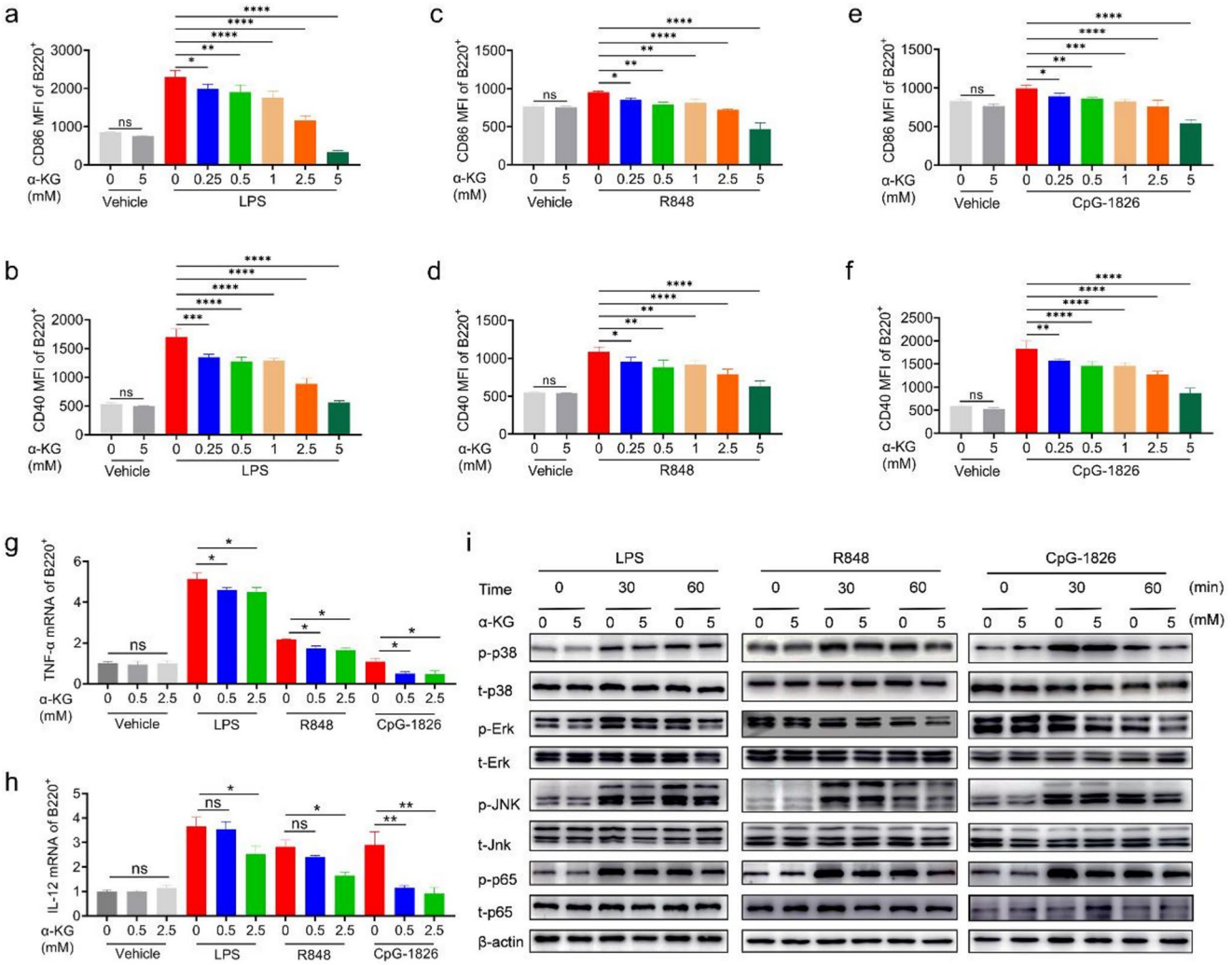

Fig. 4 α-KG suppresses the TLR-mediated activation of B cells in vitro Murine naïve B cells, isolated from the spleens of WT mice, were treated with α-KG (0, 0.25, 0.5, 1, 2.5, and 5mM) for 18 h following stimulation with LPS (100 ng/ml), R848 (1 μg/ml), and CpG-1826 (1 μM). **a-f** Flow cytometry analysis was conducted to determine the expression of CD86 and CD40 on B cells stimulated with LPS (**a**, **b**), R848 (**c**, **d**), and CpG-1826 (**e**, **f**). **g**, **h** Q-PCR was performed to measure the mRNA levels of TNF-α (**g**) and IL-12 (**h**) in B cells. **i** Western blot analysis of the phosphorylation levels of p38, Erk, JNK, and p65 after R848 treatment for 30 and 60 min, using β-actin as a loading control. The data are shown as the means ± SEM and are representative of three independent experiments. *$p<0.05$, **$p<0.01$, ***$p<0.001$, and ****$p<0.0001$ (two-tailed Student's *t*-test or ANOVA tests)

responses. Given this critical function of CD39, we hypothesized that the inhibitory effect of α-KG on TLR pathway activation may depend on the upregulation of the expression of CD39. To investigate the role of CD39 in regulating the TLR-induced activation of B cells, we crossed ENTPD1$^{fl/fl}$ mice with CD19-cre mice to obtain ENTPD1 B-cell-conditional KO (ENTPD1$^{\Delta CD19}$) mice. Splenic naïve B cells isolated from ENTPD1$^{fl/fl}$ and ENTPD1$^{\Delta CD19}$ mice were stimulated with LPS, R848, or CpG-1826, after which the activation of B cells was detected. The deletion of ENTPD1 significantly increased the TLR-mediated expression of CD86 and CD40 in B cells (Fig. 5j-o). This finding suggested that CD39 plays a negative regulatory role in the activation of TLR signaling pathways. CD39 plays an immunosuppressive role by serving as a rate-limiting enzyme in the generation of immunosuppressive adenosine (ADO). We also investigated the effect of ADO on the TLR-mediated activation of B cells. Expectedly, our findings showed that ADO strongly suppressed TLR-mediated activation of B cells (Fig. S8a-f), indicating that CD39 modulates the activation of TLR signaling pathways through a mechanism in which ADO mediates the process.

To determine whether α-KG inhibits the activation of TLR pathways by upregulating CD39, murine naïve B cells isolated from ENTPD1$^{fl/fl}$ and ENTPD1$^{\Delta CD19}$ mice were pretreated with α-KG and then stimulated with LPS, R848, and CpG-1826. Although α-KG significantly decreased TLR-mediated activation of B cells from ENTPD1$^{fl/fl}$ mice,

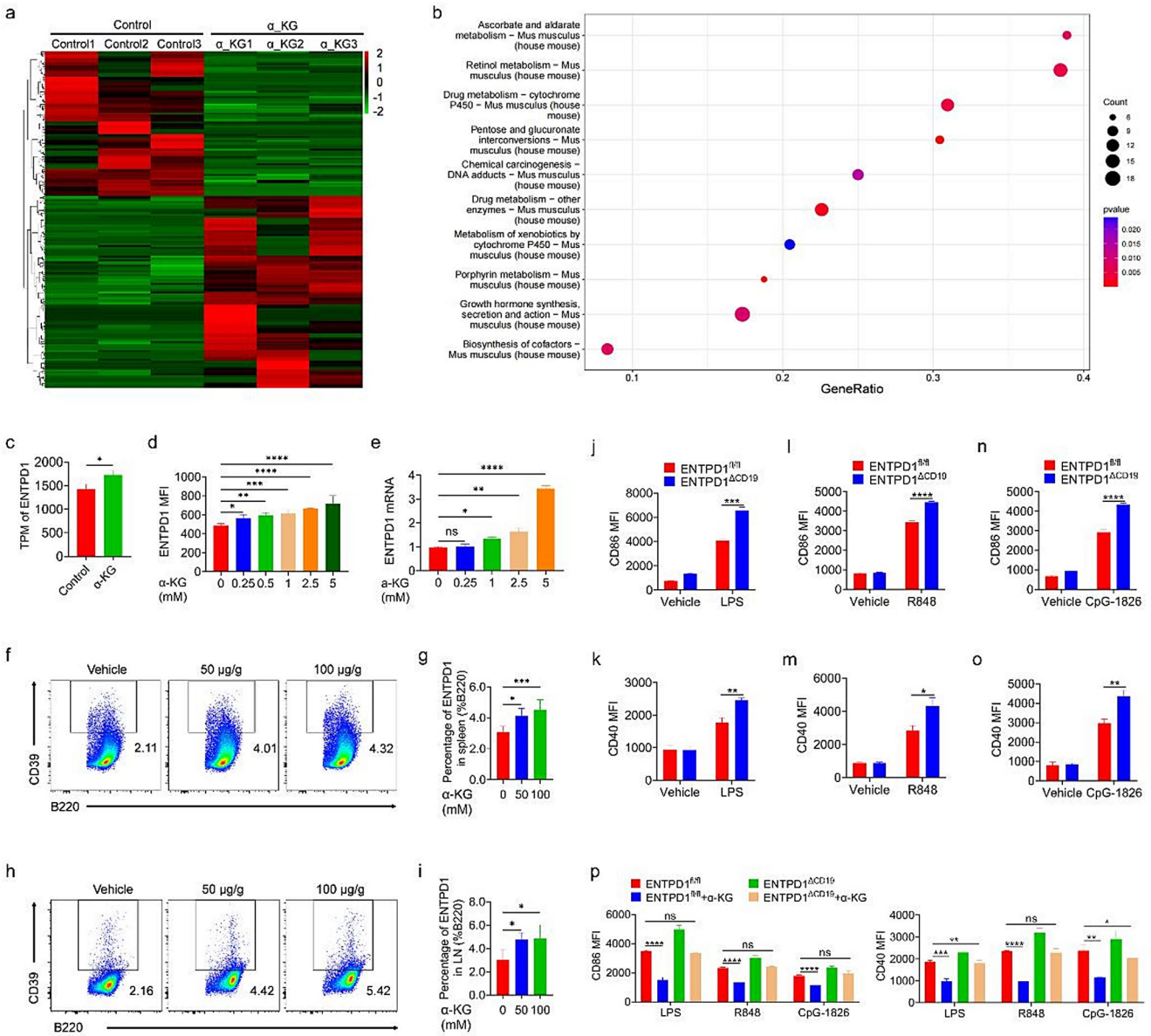

Fig. 5 α-KG inhibits the TLR-mediated activation of B cells by upregulating ENTPD1 expression **a-c** Murine splenic B cells were treated with vehicle or α-KG (5 mM) for 6 h and then RNA-seq analysis was performed. **a** Gene enrichment analysis of differential expression genes in α-KG-treated B cells versus vehicle-treated B cells. **b** KEGG signaling pathway enrichment analysis of differential gene expression in α-KG-treated B cells versus vehicle-treated B cells. **c** The values of Transcripts Per Million (TPM) of ENTPD1 gene in α-KG-treated B cells versus vehicle-treated B cells. **d** Murine splenic B cells were treated with vehicle or α-KG (0, 0.25, 0.5, 1, 2.5, and 5 mM) for 18 h and then the expression of CD39 was analyzed by flow cytometry. **e** Murine splenic B cells were treated with vehicle or α-KG (0, 0.25, 1, 2.5, and 5 mM) for 6 h and then the mRNA level of CD39 was analyzed by Q-PCR. **f-i** WT mice were treated with α-KG (50 and 100 μg/g, intraperitoneally) or vehicle for 2 weeks (twice/week), and then the expression of CD39 on B cells from spleens (**f**, **g**) and mLNs (**h**, **i**) was detected by flow cytometry. **j-o** Splenic naïve B cells, isolated from ENTPD1$^{fl/fl}$ and ENTPD1$^{\Delta CD19}$ mice, were stimulated with LPS (100 ng/ml), R848 (1 μg/ml), and CpG-1826 (1 μM) for 24 h and then the expression of CD86 and CD40 on B cells stimulated with LPS (**j**, **k**), R848 (**l**, **m**), and CpG-1826 (**n**, **o**) was detected by flow cytometry. **p** Splenic naïve B cells, isolated from ENTPD1$^{fl/fl}$ and ENTPD1$^{\Delta CD19}$ mice, were pretreated with α-KG (5 mM) followed by stimulation with LPS (100 ng/ml), R848 (1 μg/ml), and CpG-1826 (1 μM) for 24 h and then the expression of CD86 and CD40 on B cells was detected by flow cytometry. The data are shown as the means ± SEM and are representative of three independent experiments. *$p<0.05$, **$p<0.01$, ***$p<0.001$, and ****$p<0.0001$ (two-tailed Student's *t*-test or ANOVA tests)

the inhibitory effect of α-KG on TLR-mediated activation of B cells from ENTPD1$^{\Delta CD19}$ mice was notably mitigated (Fig. 5p). This observation indicated that, at least partially, α-KG exerts its inhibitory effect on TLR-mediated activation of B cells by promoting CD39 expression.

B-cell-specific deletion of CD39 contributed to the pathogenesis of lupus

Since CD39 plays a negative role in regulating the TLR-mediated activation of B cells in vitro, we next investigated whether CD39 can regulate the activation and differentiation of B cells and participate in the pathogenesis of lupus. As shown in Fig. 6a, compared to IMQ-treated ENTPD1$^{fl/fl}$ mice, IMQ-treated ENTPD1$^{\Delta CD19}$ mice presented significantly greater splenomegaly, higher spleen weight (Fig. 6b, c), Higher levels of dsDNA (Fig. 6d) and aggravated kidney injury (Fig. 6e). Moreover, immunofluorescence confocal microscopy examinations revealed considerably greater deposition of IgG and IgM in the glomeruli of IMQ-treated ENTPD1$^{\Delta CD19}$ mice (Fig. 6f), suggesting that B-cell-specific deletion of CD39 substantially accelerated the pathogenesis of lupus.

Next, we conducted an in-depth analysis of the activation and differentiation of B cells in the above model mice. Our results revealed significant upregulation of the expression of CD86 and CD40 on the surface of B cells in the spleens (Fig. 6g, h) and mLNs (Fig. S9a, S9b) of IMQ-treated ENTPD1$^{\Delta CD19}$ mice compared to those of IMQ-treated ENTPD1$^{fl/fl}$ mice. Moreover, compared to IMQ-treated ENTPD1$^{fl/fl}$ mice, IMQ-treated ENTPD1$^{\Delta CD19}$ mice presented significantly greater proportions of GC B cells (Fig. 6i and j, S9c, and S9d) and plasma cells (Fig. 6k and l, S9e, and S9f). These results confirmed that CD39 deletion can promote the activation and differentiation of B cells in vivo.

To summarize, our study revealed that serum α-KG levels were abnormally high in SLE patients and lupus model mice. Our findings indicated that α-KG can alleviate the pathogenesis of lupus and inhibit the activation and differentiation of B cells by promoting the expression of CD39. This study provided a new strategy for the clinical treatment of SLE (Fig. 7).

Discussion

The activation, differentiation, and function of immune cells require the participation of multiple metabolic pathways to meet the energetic and biosynthetic demands associated with these processes. Additionally, autoimmune diseases such as SLE are closely associated with dysregulated immune responses [27], suggesting that our metabolic processes may be intricately linked to the initiation and progression of SLE. In this study, we used organic acid-targeted histology to screen for α-KG, an organic acid that is abnormally elevated in the serum of SLE patients. Although researchers have reported the role of α-KG in the pathogenesis of various diseases, its role in the development of SLE remains unreported. Our findings indicated that α-KG significantly inhibits TLR-mediated activation and differentiation of B cells by promoting CD39 expression, thereby attenuating the progression of lupus. This observation suggested that the elevated levels of α-KG observed in SLE patients may represent a protective feedback mechanism. We hypothesized that the elevated levels of α-KG in these patients may not be sufficient to effectively inhibit the activation of immune cells, such as B cells. This observation indicates that further in-depth investigation is needed to elucidate the complex interplay between α-KG and immune cell activation in the context of SLE.

As an intermediate metabolite of the TCA cycle [28], α-KG is involved in several cellular metabolic processes, including energy metabolism, elimination of metabolic waste, and regulation of epigenetic mechanisms [29–31]. α-KG inhibits key enzymes associated with glycolysis and glutaminolysis, thereby altering chromatin accessibility and exerting antitumor effects [30]. It also exerts anti-inflammatory effects by decreasing the secretion of proinflammatory cytokines, thus playing a significant role in various pathological processes. However, the effect of α-KG on autoimmune diseases, particularly its involvement in the pathogenesis of SLE, remains poorly understood. In this study, we showed for the first time that α-KG significantly improved conditions in MRL/*lpr* mice as well as in an IMQ-induced lupus model. Additionally, α-KG inhibited the activation and differentiation of immune cells, particularly B cells, in lupus-affected mice. The underlying molecular mechanism may involve the inhibition of TLR signaling pathways that mediate immune cell activation and differentiation, thus delaying the onset and progression of SLE.

Fig. 6 B-cell-specific deletion of CD39 substantially accelerates the disease development of IMQ-induced lupus-prone mice ENTPD1$^{fl/fl}$ mice and ENTPD1$^{\Delta CD19}$ mice (female, eight-week-old) were treated with IMQ for ten weeks (three times per week). **a** The graph illustrates the disease progression in ENTPD1$^{fl/fl}$ mice or ENTPD1$^{\Delta CD19}$ mice following IMQ induction. **b** Representative image of the spleen, **c** spleen weights, **d** serum levels of anti-dsDNA antibody, **e** H&E staining of kidneys, **f** renal IgG and IgM deposition in IMQ-treated ENTPD1$^{fl/fl}$ mice and ENTPD1$^{\Delta CD19}$ mice. **g-l** Flow cytometry was performed to detected the expression of CD86 and CD40 on B220^{+} B cells (**g**, **h**), the percentage of GC B cells (B220^{+}GL7^{+}CD95^{+}) in B220^{+} B cells (**i**, **j**), and the percentage of plasma cells (CD138^{+}) (**k**, **l**) in the spleens. The data are shown as the means ± SEM and are representative of three independent experiments ($n = 6$ mice/group). *$p < 0.05$, **$p < 0.01$, and ***$p < 0.001$ (two-tailed Student's *t*-test or ANOVA tests)

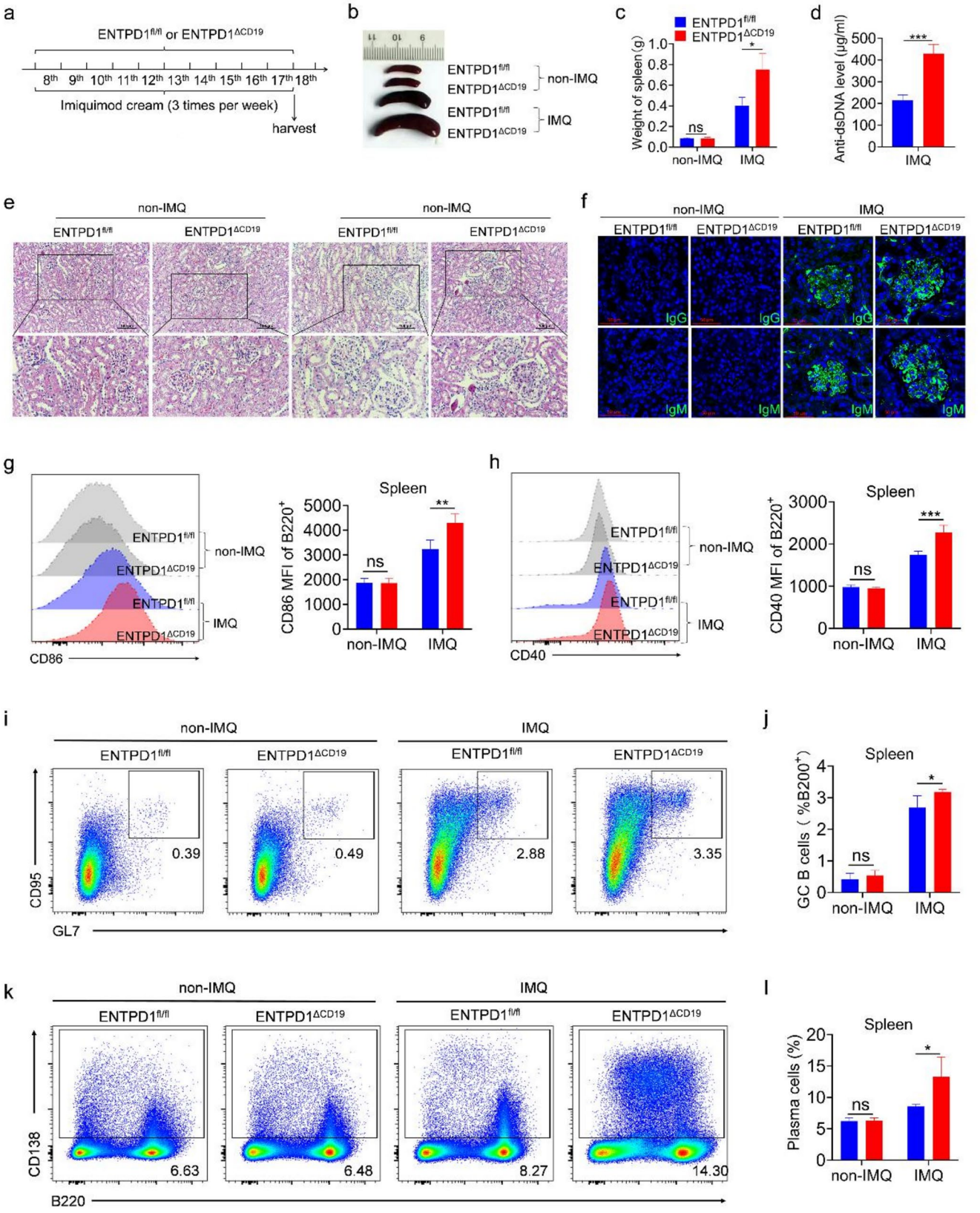
a
ENTPD1fl/fl or ENTPD1ΔCD19
8th 9th 10th 11th 12th 13th 14th 15th 16th 17th 18th
Imiquimod cream (3 times per week)
harvest
b
ENTPD1fl/fl
ENTPD1ΔCD19
non-IMQ
ENTPD1fl/fl
ENTPD1ΔCD19
IMQ
c
ENTPD1fl/fl
ENTPD1ΔCD19
Weight of spleen (g)
ns
*
non-IMQ
IMQ
d
Anti-dsDNA level (μg/ml)
***
IMQ
e
non-IMQ
non-IMQ
ENTPD1fl/fl
ENTPD1ΔCD19
ENTPD1fl/fl
ENTPD1ΔCD19
f
non-IMQ
IMQ
ENTPD1fl/fl
ENTPD1ΔCD19
ENTPD1fl/fl
ENTPD1ΔCD19
IgG
IgM
g
ENTPD1fl/fl
ENTPD1ΔCD19
non-IMQ
ENTPD1fl/fl
ENTPD1ΔCD19
IMQ
CD86
Spleen
CD86 MFI of B220+
**
ns
non-IMQ
IMQ
h
ENTPD1fl/fl
ENTPD1ΔCD19
non-IMQ
ENTPD1fl/fl
ENTPD1ΔCD19
IMQ
CD40
Spleen
CD40 MFI of B220+
***
ns
non-IMQ
IMQ
i
non-IMQ
IMQ
ENTPD1fl/fl
ENTPD1ΔCD19
ENTPD1fl/fl
ENTPD1ΔCD19
0.39
0.49
2.88
3.35
CD95
GL7
j
Spleen
GC B cells (%B200+)
*
ns
non-IMQ
IMQ
k
non-IMQ
IMQ
ENTPD1fl/fl
ENTPD1ΔCD19
ENTPD1fl/fl
ENTPD1ΔCD19
6.63
6.48
8.27
14.30
CD138
B220
l
Spleen
Plasma cells (%)
*
ns
non-IMQ
IMQ

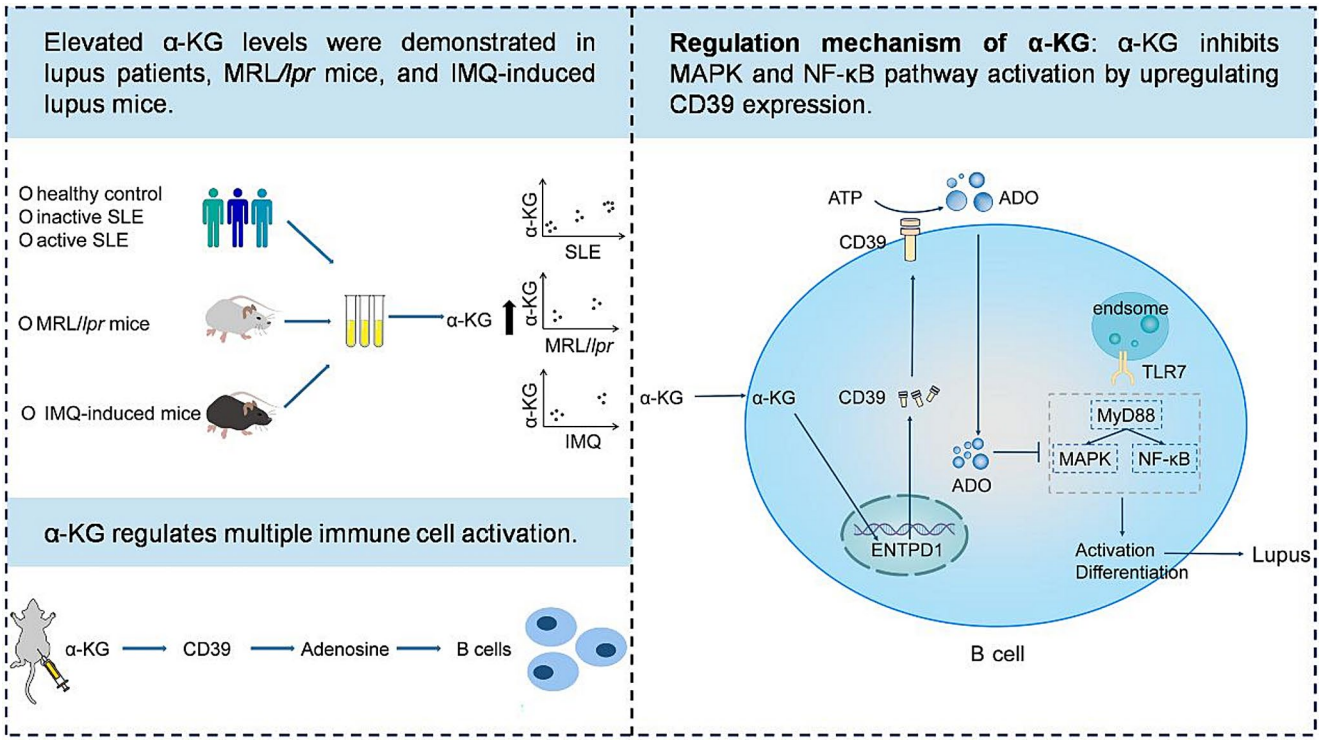

Fig. 7 α-KG mitigates the pathogenesis of lupus by enhancing CD39 expression to inhibits the activation and differentiation of B cells

Abnormal differentiation and activation of T cells greatly influence the pathogenesis of SLE. Our findings revealed that α-KG treatment strongly inhibited the activation of T cells, as well as the differentiation of Tfh cells and memory $CD4^+$ T cells, in the spleens and lymph nodes of lupus-prone mice. These results suggested that α-KG may exert a direct or indirect regulatory influence on the activation and differentiation of T cells. α-KG may play a role in modulating the initiation and progression of T cell-mediated diseases. However, because this study focused on B cells, we did not examine the regulatory role of α-KG in the activation and differentiation of T cells. We acknowledge that our study focused solely on plasma cell percentages and did not quantify absolute cell numbers, representing a limitation. Future studies will incorporate absolute cell number measurements to provide a more comprehensive dataset.

Both in vivo and in vitro experiments showed that α-KG can effectively alleviate the progression of SLE and inhibit the activation and differentiation of immune cells by preventing the activation of TLR pathways. Thus, we hypothesized that α-KG may also have therapeutic effects on the pathogenesis of TLR-related diseases; however, additional studies are needed to further validate this hypothesis. We found that α-KG inhibited the TLR-mediated activation of B cells by increasing the expression of CD39. Previous studies have shown that CD39 is involved in the production of extracellular ADO through ATP metabolism. Our findings further revealed that ADO could significantly inhibit TLR-mediated activation of immune cells, as indicated by a decrease in the expression of CD86 and CD40. Our in vitro experiments demonstrated that ENTPD1 deficiency markedly reverses the inhibitory effects of α-KG on TLR-mediated B cell activation. Meantime, in vivo studies confirmed that α-KG significantly ameliorates disease progression in lupus-prone mice, while ENTPD1 deficiency exacerbates SLE pathogenesis. These findings collectively support the hypothesis that α-KG alleviates SLE by upregulating ENTPD1 expression, thereby suppressing B cell activation. Furthermore, while our study primarily focused on the role of α-KG in regulating B cell activation and differentiation through CD39 upregulation, we acknowledge that CD39 is also expressed in other immune cell populations, such as macrophages and dendritic cells, where it plays a critical role in immune regulation. This suggests that α-KG may modulate the activation and differentiation of these immune cells through CD39 upregulation, potentially contributing to the pathogenesis of SLE. In future studies, we will further investigate whether α-KG regulates CD39 expression and function in other immune cells, as well as its role in the development of SLE.

Although we found that α-KG has therapeutic effects on lupus mice, further investigations into its dose-effect relationship, long-term efficacy, and safety need to be conducted before its clinical application can be considered.

Future studies may involve determining the optimal dosage of α-KG for humans, assessing the effects of long-term α-KG supplementation, and investigating potential synergistic effects when α-KG is combined with other therapeutic interventions. These studies may provide a more comprehensive understanding of the role of α-KG in the treatment of SLE and utilize its therapeutic potential more effectively.

To summarize, in this study, we determined the effect of α-KG on the pathogenesis of lupus, establishing a framework for the potential clinical application of α-KG in SLE treatment. We also found that α-KG can suppress the TLR-mediated activation of immune cells. Further studies on the function of α-KG may provide a theoretical basis for developing effective strategies for treating autoimmune diseases.

Supplementary Information The online version contains supplementary material available at https://doi.org/10.1007/s00018-025-05734-5.

Acknowledgements Not applicable.

Author contributions All authors contributed to the study's conception and design. YHY, HBX, and GJD engaged in study design and coordination and material support for obtained funding and supervised the study. YZG, YCX, YXH, LY, JKL, ZYZ, and TQZ performed most of the experiments and statistical analyses and wrote the manuscript. SZ and LLZ performed parts of the experiments. All authors reviewed and andapproved the final manuscript.

Funding This work was supported by National Natural Science Foundation of China (82471834, 82071824), Tai Shan Young Scholar Foundation of Shandong Province (tsqn202211234), Shandong Provincial Natural Science Foundation (ZR2024MH279), Shandong Provincial Youth Innovation Technology Support Program (2021KJ074), and Jining medical university high-level scientific research project cultivation plan (JYGC2022KJ005).

Data availability Data will be made available on request.

Declarations

Ethics approval and consent to participate The authors declare their commitment to the Helsinki Declaration of Ethical Principles for Medical Research Involving Human Subjects and confirm consent was obtained from each participant, ensuring adherence to ethical guidelines. The study protocol received approval from the Medical Ethics Committee of Jining Medical College under the reference number JNMC-2022-YX-006. All mouse experiments adhered to the guidelines for animal care and were conducted in accordance with the protocols approved by the Animal Care Committee of Jining Medical University (JNMC-2024-DW-101).

Conflict of interest The authors declare that they have no known competing financial interests or personal relationships that could have appeared to influence the work reported in this paper.

References

1. Tsokos GC (2024) The immunology of systemic lupus erythematosus. Nat Immunol 25:1332–1343. https://doi.org/10.1038/s41590-024-01898-7
2. Siegel CH, Sammaritano LR (2024) Systemic lupus erythematosus: A review. JAMA 331:1480. https://doi.org/10.1001/jama.2024.2315
3. Arnaud L, Chasset F, Martin T (2024) Immunopathogenesis of systemic lupus erythematosus: an update. Autoimmun Rev 23:103648. https://doi.org/10.1016/j.autrev.2024.103648
4. Schett G, Nagy G, Krönke G, Mielenz D (2024) B-cell depletion in autoimmune diseases. https://doi.org/10.1136/ard-2024-225727. Ann Rheum Dis ard-2024-225727
5. Takeshima Y, Iwasaki Y, Nakano M et al (2022) Immune cell multiomics analysis reveals contribution of oxidative phosphorylation to B-cell functions and organ damage of lupus. Ann Rheum Dis 81:845–853. https://doi.org/10.1136/annrheumdis-2021-221464
6. Yang M, Long D, Hu L et al (2021) AIM2 deficiency in B cells ameliorates systemic lupus erythematosus by regulating Blimp-1–Bcl-6 axis-mediated B-cell differentiation. Sig Transduct Target Ther 6:341. https://doi.org/10.1038/s41392-021-00725-x
7. Kawai T, Ikegawa M, Ori D, Akira S (2024) Decoding Toll-like receptors: recent insights and perspectives in innate immunity. Immunity 57:649–673. https://doi.org/10.1016/j.immuni.2024.03.004
8. Hamerman JA, Barton GM (2024) The path ahead for Understanding Toll-like receptor-driven systemic autoimmunity. Curr Opin Immunol 91:102482. https://doi.org/10.1016/j.coi.2024.102482
9. Fillatreau S, Manfroi B, Dörner T (2021) Toll-like receptor signalling in B cells during systemic lupus erythematosus. Nat Rev Rheumatol 17:98–108. https://doi.org/10.1038/s41584-020-00544-4
10. Brown GJ, Cañete PF, Wang H et al (2022) TLR7 gain-of-function genetic variation causes human lupus. Nature 605:349–356. https://doi.org/10.1038/s41586-022-04642-z
11. Liu S, Lagos J, Shumlak NM et al (2024) NADPH oxidase exerts a B cell–intrinsic contribution to lupus risk by modulating endosomal TLR signals. J Exp Med 221:e20230774. https://doi.org/10.1084/jem.20230774
12. Soni C, Wong EB, Domeier PP et al (2014) B Cell–Intrinsic TLR7 signaling is essential for the development of spontaneous germinal centers. J Immunol 193:4400–4414. https://doi.org/10.4049/jimmunol.1401720
13. Jenks SA, Cashman KS, Zumaquero E et al (2018) Distinct effector B cells induced by unregulated Toll-like receptor 7 contribute to pathogenic responses in systemic lupus erythematosus. Immunity 49:725–739e6. https://doi.org/10.1016/j.immuni.2018.08.015

14. Xiao Y, Hu Y, Gao Y et al (2024) IL-17B alleviates the pathogenesis of systemic lupus erythematosus by inhibiting FASN-mediated differentiation of B cells. JCI Insight 9:e181906. https://doi.org/10.1172/jci.insight.181906
15. Chapman NM, Chi H (2022) Metabolic adaptation of lymphocytes in immunity and disease. Immunity 55:14–30. https://doi.org/10.1016/j.immuni.2021.12.012
16. Asadi Shahmirzadi A, Edgar D, Liao C-Y et al (2020) Alpha-Ketoglutarate, an endogenous metabolite, extends lifespan and compresses morbidity in aging mice. Cell Metabol 32:447–456e6. https://doi.org/10.1016/j.cmet.2020.08.004
17. Chin RM, Fu X, Pai MY et al (2014) The metabolite α-ketoglutarate extends lifespan by inhibiting ATP synthase and TOR. Nature 510:397–401. https://doi.org/10.1038/nature13264
18. Gyanwali B, Lim ZX, Soh J et al (2022) Alpha-Ketoglutarate dietary supplementation to improve health in humans. Trends Endocrinol Metabolism 33:136–146. https://doi.org/10.1016/j.tem.2021.11.003
19. Liu S, Yang J, Wu Z (2021) The regulatory role of α-Ketoglutarate metabolism in macrophages. Mediat Inflamm 2021:1–7. https://doi.org/10.1155/2021/5577577
20. Zasłona Z, O'Neill LAJ (2020) Cytokine-like roles for metabolites in immunity. Mol Cell 78:814–823. https://doi.org/10.1016/j.molcel.2020.04.002
21. Milanović M, Bekić M, Đokić J et al (2024) Exogenous α-ketoglutarate modulates redox metabolism and functions of human dendritic cells, altering their capacity to polarise T cell response. Int J Biol Sci 20:1064–1087. https://doi.org/10.7150/ijbs.91109
22. Liu GM, Lu JJ, Sun WX et al (2023) Dietary alpha-ketoglutarate enhances intestinal immunity by *Th17/Treg* immune response in piglets after lipopolysaccharide challenge. J Anim Sci 101:skad213. https://doi.org/10.1093/jas/skad213
23. Weisshaar N, Ma S, Ming Y et al (2023) The malate shuttle detoxifies ammonia in exhausted T cells by producing 2-ketoglutarate. Nat Immunol 24:1921–1932. https://doi.org/10.1038/s41590-023-01636-5
24. Liang G, Hu J, Liu R et al (2024) α-Ketoglutarate plays an inflammatory inhibitory role by regulating scavenger receptor class a expression through N6-methyladenine methylation during sepsis. Eur J Immunol 2350655. https://doi.org/10.1002/eji.202350655
25. Montano EN, Bose M, Huo L et al (2024) α-Ketoglutarate–Dependent KDM6 histone demethylases and Interferon-Stimulated gene expression in lupus. Arthritis Rheumatol Art 42724. https://doi.org/10.1002/art.42724
26. Patel CH, Leone RD, Horton MR, Powell JD (2019) Targeting metabolism to regulate immune responses in autoimmunity and cancer. Nat Rev Drug Discov 18:669–688. https://doi.org/10.1038/s41573-019-0032-5
27. Huang F, Luo X, Ou Y et al (2023) Control of histone demethylation by nuclear-localized α-ketoglutarate dehydrogenase. Science 381:eadf8822. https://doi.org/10.1126/science.adf8822
28. Wagner M, Bertero E, Nickel A et al (2020) Selective NADH communication from α-ketoglutarate dehydrogenase to mitochondrial transhydrogenase prevents reactive oxygen species formation under reducing conditions in the heart. Basic Res Cardiol 115:53. https://doi.org/10.1007/s00395-020-0815-1
29. Bian K, Lenz SAP, Tang Q et al (2019) DNA repair enzymes ALKBH2, ALKBH3, and AlkB oxidize 5-methylcytosine to 5-hydroxymethylcytosine, 5-formylcytosine and 5-carboxylcytosine in vitro. Nucleic Acids Res 47:5522–5529. https://doi.org/10.1093/nar/gkz395
30. Parker JL, Kato T, Kuteyi G et al (2023) Molecular basis for selective uptake and elimination of organic anions in the kidney by OAT1. Nat Struct Mol Biol 30:1786–1793. https://doi.org/10.1038/s41594-023-01039-y
31. Chung C, Sweha SR, Pratt D et al (2020) Integrated metabolic and epigenomic reprograming by H3K27M mutations in diffuse intrinsic Pontine gliomas. Cancer Cell 38:334–349e9. https://doi.org/10.1016/j.ccell.2020.07.008